

# UCSB METHOD FOR BROADBAND GROUND MOTION FROM KINEMATIC SIMULATIONS OF EARTHQUAKES

RALPH ARCHULETA AND JORGE CREMPIEN

## Release Notes (V. 19.4)

### 1. High frequency simulation code

We have modified the 1D frequency/wavenumber code of Zhu and Rivera (2002) to include frequency dependent  $Q$ . We also noticed that the amplitude of high-frequency (HF) waves calculated with typical 1D layered velocity structures decrease much quicker than  $1/r$ ,  $r$  is distance (Crempien and Archuleta, 2014). In this update, we compute HF Green's functions from a homogeneous half-space with P- and S-wave values taken just above the Moho discontinuity. The amplitudes of HF Green's functions are increased at different frequencies using the quarter wavelength amplification method (QWAM; Boore and Joyner, 1997) and their waveforms are shifted to be consistent with S wave arrivals of low-frequency calculations (Crempien and Archuleta, 2015).

### 2. Source generator

Following Gusev (2011), we add the rupture time  $T(\xi)$  at the fault site  $\xi$  with an additional perturbation  $\Delta\tau(\xi)$ .  $\Delta\tau(\xi)$  is a random field, with zero mean and a fractal spatial distribution with a power spectrum proportional to  $k^{-d}$  ( $k$  is the wavenumber). We used  $d$  values of 1.0 in the Fourier domain.

## Method overview

UCSB method uses representation theorem (Aki and Richards, 1980) to calculate the ground motion from a kinematic source model consistent with a dynamic rupture. Both low-frequency and high-frequency ground motions are calculated with same source, but with different synthetic approaches. At frequencies below 1 Hz, 1D and 3D synthetic algorithms are adopted to generate exact earth response for the given velocity model. At frequencies above 1 Hz, 1D synthetic algorithm is adopted to compute Green's functions from a pseudo half-space model with the speeds of P- and S-waves values just above the Moho discontinuity. The amplitudes of calculated HF Green's function are modified at different frequencies using the quarter wavelength amplification method of Boore and Joyner (1997) and their waveforms are shifted to be consistent with S wave arrivals of low-frequency calculations (Crempien and Archuleta, 2015). The two responses are then combined together to produce a single time history using the wavelet domain approach of Liu et al. (2006). The method was originally developed by Liu et al. (2006). Schmedes et al. (2009, 2010, 2013) regressed the relations among autocorrelations of slip and other source parameters, using the results of 300 dynamic simulations. Crempien and Archuleta (2015) improved the modeling of high frequency ground motion.

UCSB method uses an analytic slip rate function  $\dot{s}(\xi, \tau)$ ,  $\xi$  and  $\tau$  denotes the location on the fault plane and time of rupture, to define the scenario source rupture of an earthquake with given magnitude. Several analytic slip rate functions can be selected. To specify the source requires knowing four parameters at each point on the fault: slip, start time (rupture time), peak time and rise time. The amplitude of the slip is determined from a truncated Cauchy distribution (Lavallée et al., 2006), which implements the scaling relationship between maximum slip and magnitude (McGarr and Fletcher, 2003). The spatial distribution of the slip function is determined by choosing a slope of the autocorrelation of the 2D power spectral density in wavenumber (Liu et al., 2009). The power spectrum is then chosen to be von Karman with the correlation length taken from Mai and Beroza (2002). The slope of the 2D autocorrelation for the rupture time, peak time and rise time are linearly related to the slope of the autocorrelation for slip (Figure 1, Schmedes et al., 2013). Finally, the distributions of the rupture time, rise time, and peak time are perturbed so that the cumulative moment rate spectrum of the entire fault matches a Brune spectrum with a given corner frequency—the second global parameter related to the earthquake besides the magnitude.

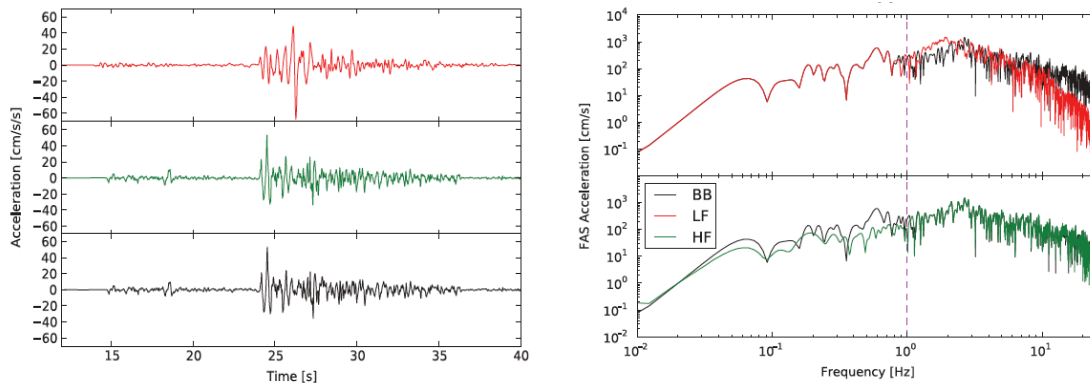


Figure 1. Combining low-frequency (LF) and high-frequency (HF; depicted in red and green lines, respectively) seismograms to form a broadband (BB) seismogram (black line) at a distance of  $R_{rup} \approx 82$  km from the source. For frequencies less than 1.0 Hz, the BB Fourier amplitude spectrum (FAS) overlays almost identically the LF FAS; from 1.0 to 25 Hz, the BB FAS is almost identical to the HF FAS. (Crempien and Archuleta, 2015).

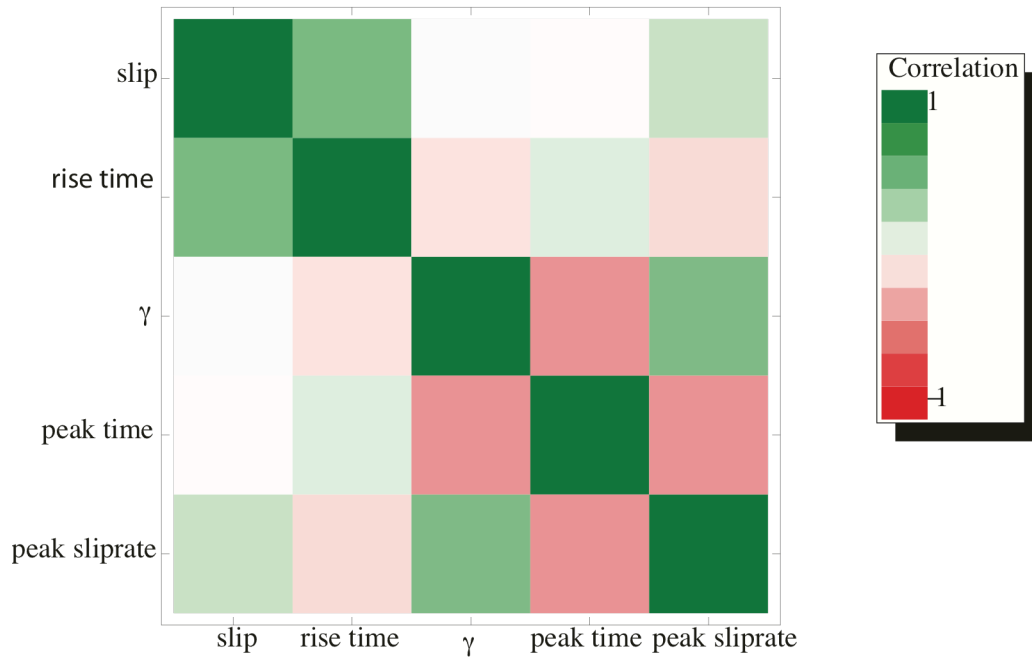


Figure 2: Correlation matrix between the parameters on the fault (Schmedes et al., 2013). This correlation is enforced in the UCSB method of computing ground motions from kinematic simulations of earthquakes.

Tables of Parameters

<b>Fixed Parameters</b>		
<b>Fault</b>	<b>Earthquake</b>	<b>Green's Function</b>
Length	Seismic Moment	P and S Wave Velocity (z)
Width	Hypocenter	Density (z)
Dip		Attenuation (z): $Q_0$ and $\alpha$ where $Q = Q_0 f^\alpha$
Rake		Maximum Frequency
Strike		
Depth to Top of Fault		

<b>Parameters—Can Be Changed with Each Simulation</b>			
<b>Fault</b>	<b>Earthquake</b>	<b>Kinematic Parameters</b>	<b>Path and Site</b>
dL (grid size along strike and dip)	Corner Frequency—determines the stress drop when combined with seismic moment	Autocorrelation of slip $v_{FS}(slip)$ Will automatically affect peak time, rise time and rupture velocity	Kappa
dW (grid size down dip)	Hypocenter	Gusev parameter	
No. of extra points within subfault	Variation of Dip		
Taper on slip at the edges of fault	Variation of Rake		
Taper on rupture velocity at the edges of fault	Variation of Strike		

## REFERENCES:

- Aki, K. and P. G. Richards (1980). *Quantitative Seismology: Theory and Methods*, Vol. I, W. H. Freeman and Co., New York, 557 pp.
- Gusev, A. A. (2011). Broadband kinematic stochastic simulation of an earthquake source: A refined procedure for application in seismic hazard studies, *Pure Appl. Geophys.*, **168**, 155–200, DOI: 10.1007/s00024-010-0156-3.
- Crempien, J. G. F., and R. J. Archuleta (2014). Does a 1D velocity structure hurt or help ground motion predictions? *Seismol. Res. Lett.*, **85**(2), 508.
- Crempien and Archuleta (2015). UCSB method for simulation of broadband ground motion from kinematic earthquake sources, *Seismol. Res. Lett.*, **86**(1), 61-67. DOI: 10.1785/0220140103.
- Lavallée, D., P. Liu, and R. J. Archuleta (2006), Stochastic model of heterogeneity in earthquake slip spatial distributions, *Geophys. J. Int.*, **165**, 622-640.
- Liu, P. and R. J. Archuleta (2006). Efficient modeling of Q for 3D numerical simulation of wave propagation, *Bull. Seismol. Soc. Am.*, **96** (4), 1352-1351, doi: 10.1785/0120050173.
- Liu, P., R. J. Archuleta and S. H. Hartzell (2006). Prediction of broadband ground-motion time histories: Hybrid low/high-frequency method with correlated random source parameters, *Bull. Seismol. Soc. Am.*, **96**(6), 2118-2130, doi: 10.1785/0120060036.
- Mai, P. M., and G. C. Beroza (2002). A spatial random field model to characterize complexity in earthquake slip, *J. Geophys. Res.*, **107**(B11), 2308, doi:10.1029/2001JB000588.
- McGarr, A. and J. B. Fletcher (2003). Maximum slip in earthquake fault zones, apparent stress, and stick-slip friction, *Bull. Seismol. Soc. Am.*, **93**(6), 2355–2362.
- Schmedes, J. (2009). Kinematic and dynamic modeling of the earthquake source: On spatial correlations of source parameters, supershear transition, and strong ground motion, PhD Dissertation, University of California, Santa Barbara, 231 p.
- Schmedes, J., R. J. Archuleta, and D. Lavallée (2010). Correlation of earthquake source parameters inferred from dynamic rupture simulations, *J. Geophys. Res.*, **115**, B03304, DOI:10.1029/2009JB006689.
- Schmedes, J., R. J. Archuleta, and D. Lavallée (2013). A kinematic rupture model generator incorporating spatial interdependency of earthquake source parameters, *Geophys. J. Int.* **192** (3), 1116-1131. DOI: 10.1093/gji/ggs02.
- Zhu, L. and L. A. Rivera (2002). A note on the dynamic and static displacements from a point source in multilayered media, *Geophys. J. Int.*, **148**, 619–627.